

Article

Silicon Substrate Treated with Diluted NaOH Aqueous for Si/PEDOT: PSS Heterojunction Solar Cell with Performance Enhancement

Tao Chen ^{1,2}, Hao Guo ², Leiming Yu ^{1,2}, Tao Sun ² and Yu Yang ^{2,*}

¹ School of Physics and Astronomy, Yunnan University, Kunming 650091, China; taochen008@ynu.edu.cn (T.C.); yuleiming@mail.ynu.edu.cn (L.Y.)

² International Joint Research Center for Optoelectronic and Energy Materials, School of Materials and Energy, Yunnan University, Kunming 650091, China; guohao2408@mail.ynu.edu.cn (H.G.); t.sun@griffith.edu.au (T.S.)

* Correspondence: yuyang@ynu.edu.cn

Received: 6 August 2020; Accepted: 1 September 2020; Published: 8 September 2020



Abstract: Si/PEDOT: PSS solar cell is an important alternative for photovoltaic device due to its anticipated high theoretical efficiency and simple manufacturing process. In this study, processing silicon substrate with diluted NaOH aqueous solution was found to be an effective method for improving device performance, one that notably improves junction quality and light trapping ability. When immersed in diluted NaOH aqueous solution, the junction quality was improved according to the enlarged fill factor, reduced series resistance, and enhanced minor carrier lifetime. The diluted NaOH aqueous solution immersion etched the silicon surface and helped with the enhancement of light trapping ability, further improving the short-circuit current density. Although diluted NaOH aqueous solution immersion for bare silicon could improve the performance of devices, proper immersion time was needed. The influence of immersion time on device performances was investigated. The photovoltaic conversion efficiency easily increased from 10.01% to 12.05% when silicon substrate was immersed in diluted NaOH aqueous for 15 min. This study contributes to providing efficient and convenient methods for preparing high performance Si/PEDOT: PSS solar cells.

Keywords: Si/PEDOT: PSS solar cell; NaOH aqueous; surface modification; optical-electro characteristics; short-circuit current

1. Introduction

Solar energy is the inevitable choice for addressing problems of energy shortage and environmental pollution. A new generation of solar cell, the silicon/poly (3,4-ethylenedioxy-thiophene): poly (styrene-sulfonate) (Si/PEDOT: PSS) solar cell was proposed considering the advantages of silicon-based solar cells and organic solar cells, including high photovoltaic conversion efficiency (PCE), low-temperature process capability, easy preparation, low cost, etc. [1]. The PCE of the Si/PEDOT: PSS solar cell has been improved 17.4% since its inception [2]; considerable room for further improvement still exists [3,4]. One of the essential problems that restricted the further improvement of PCE was the poor interface contact between Si and PEDOT: PSS film [5], which affected the junction quality of the Si/PEDOT: PSS solar cell and further influenced device performance.

To obtain excellent interface contact, the universal approach was applied to improve the wettability of PEDOT: PSS aqueous solution on Si prior to the spin-coating [6]. Usually, incorporating a surfactant into the PEDOT: PSS aqueous solution is a simple method, and it helped to improve the PCE of the Si/PEDOT: PSS solar cell [6–10]. The most popular surfactant was p-t-octylphenol (Triton X-100), which optimizes interface contact and assists in the enhancement of PEDOT: PSS film conductivity [7,10–13],

resulting in increased PCE. Other researchers tried the fluorosurfactant Zonyl FS-300, and the PCE of the prepared device could reach 10.2% [9]. In recent years, the silane coupling agent named 3-glycidoxypropyltrimethoxydsilane (GOPS) has been incorporated into the PEDOT: PSS aqueous solution, with a proper mass ratio to optimize the interface contact, contributing to the enhancement of open-circuit voltage (V_{oc}) and the PCE of a device with nano-structured Si [14–16]. Although incorporating the surfactant, or GOPS, was an effective method to optimize the interface contact and enhance the PCE, the residual surfactant in PEDOT: PSS film would cause either mechanical properties reduction or conductivity declination [16]. Another method researchers used to optimize interface contact was to prepare the oxide layer on the Si surface to serve as the crucial interface layer. Silicon oxide (SiO_x) [17,18], aluminum oxide (Al_2O_3) [19], and titanium oxide (TiO_x) [20] were prepared on the Si surface, and showed efficiency in improving the wettability of Si and the performance of the device. However, the complex synthesis procedure and the high cost of oxide layer preparation were relatively complicated and expensive [17,19–21]. Although Zhang et al. [18] developed a convenient and low-cost method to prepare SiO_x , the much lower and more convenient device preparation processing was still needed.

The main reason for the poor interface contact of plain Si substrate heterojunction solar cells was the hydrophobic nature of the Si surface, caused by cleaning the Si substrate using RCA methods [22–24]. The Si surface terminating with hydrogen ($-H$), after being immersed in diluted HF solution, was the key reason for the highly hydrophobic nature of the Si surface and poor interface contact [18]. Thus, replacing the $-H$ with hydrophilic radicals is a new method to optimize interface contact. When the Si surface is terminated with hydroxyl ($-OH$), the wettability of the Si surface is improved [25]. Piranha solution boiling, oxygen plasma treatment [26] and application of tetramethylammonium hydroxide [14,15] were the major methods to terminate the Si surface with $-OH$. The piranha solution terminates the Si surface with $-OH$, but also introduces a thick SiO_x layer [21]. NaOH aqueous solution can also terminate the Si surface with $-OH$ and etch the Si surface at the same time [27–29], which might give rise to the performance of the Si/PEDOT: PSS solar cells. NaOH aqueous solution was widely applied to prepare nano-structured Si substrate, but few studies contributed to the further understanding of the effect of NaOH aqueous solution on Si substrate and Si/PEDOT: PSS solar cells.

In this study, both Si substrate with diluted NaOH aqueous immersion and substrate without immersion were applied to prepare the Si/PEDOT: PSS solar cells. The electrochemical impedance spectra (EIS) and carrier lifetime measurement were applied to consider the junction quality of devices. The influence of immersion time of Si substrate in diluted NaOH aqueous on device performance and the Si substrate is also presented. The results indicate that properly diluted NaOH aqueous solution processing helps to enhance performance. The test results reveal the influence of diluted NaOH aqueous solution on Si substrate and the performance of Si/PEDOT: PSS solar cells. This paper contributes an efficient and convenient method for developing high performance Si/PEDOT: PSS solar cells.

2. Materials and Methods

2.1. Materials

The resistivity and thickness of the one-side polished silicon wafers were 1–3 $\Omega\cdot\text{cm}$ and 300 μm (Hefei-Kejing Materials Technology Co., Ltd., Hefei, China). PEDOT: PSS (Clevios PH1000, Heraeus, Hanau, Germany) aqueous solution was purchased from Sigma-Aldrich (Shanghai, China). Phenyl-C61-butyric acid methyl ester (PC61BM, >99.5%) was purchased from Xi'an Polymer Light Technology (Xi'an, China). Dimethylsulfoxide (DMSO, 99.9%), sodium hydroxide (NaOH, AR), ethanol, sulfuric acid (H_2SO_4 , AR, 98%), acetone, hydrogen peroxide (H_2O_2 , AR, 30 wt % in H_2O), and hydrofluoric acid (HF, AR, $\geq 40\%$) were purchased from Yunnan-Keyi (Kunming, China).

2.2. Experiment and Device Preparation

The Si substrate with size 10×10 mm was cleaned according to the standard RCA method to remove the impurities and native SiO_x layer on its surface. Subsequently, the cleaned Si was immersed into diluted NaOH aqueous solution (0.03 mg/mL) for 5, 15, 30, 45, and 60 min, separately. Then, the Si substrate was washed with deionized water in ultrasonic cleaner for 5 min, and transferred into a glove box immediately after nitrogen drying. To improve the electrical conductivity of the PEDOT: PSS film, the PEDOT: PSS aqueous solution was doped with DMSO (mass ratio of DMSO was 5 wt %) and assisted by ultrasonic treatments for 2 h. PC61BM was dissolved in chlorobenzene with a concentration of 20 mg/mL. The PEDOT: PSS/DMSO solution was spin-coated on the front (polished) side of the Si substrate with a speed of 3000 rpm for 60 s, and annealed for 30 min at 130°C . The PC61BM film on the rear side of the Si substrate was also spin-coated at a speed of 2000 rpm for 40 s, and annealing temperature and time were 120°C and 20 min, respectively. Then, the substrate was cooled to environment temperature. The PEDOT: PSS/Si/PC61BM samples were then transferred into vacuum evaporating instruments to prepare a 200 nm silver (Ag) grid and a 100 nm aluminum (Al) film. For convenient discussion, the prepared devices were named solar/-OH(5), solar/-OH(15), solar/-OH(30), solar/-OH(45), and solar/-OH(60), and the device that was not processed with diluted NaOH aqueous solution was named solar/-H.

2.3. Characterizations

The current density–voltage (J–V) curve of the Si/PEDOT: PSS solar cells was measured by a Keithley 2400 (Tektronix Inc., Beaverton, OR, USA) under the simulated solar illumination (AM 1.5 Global solar simulator) with an intensity of 100 mW/cm^2 (calibrated by a standard monocrystalline silicon solar cell). Atomic force microscopy (SPA-400, Seiko Instruments, Chiba, Japan) was applied to study the surface morphology of Si substrates. External quantum efficiency (EQE) measurements were recorded with a quantum efficiency measurement system (SCS10, Zolix, Beijing, China). The EIS measurement was recorded via an electrochemical workstation (model 660D, Shanghai Chen Hua Instrument Co., Ltd., Shanghai, China), and used in dark conditions in a frequency range of 10^{-1} – 10^5 Hz with a DC bias of 0 V. The reflectance of the Si substrates was measured using a spectrophotometer (UV-3600Plus, Shimadzu, Kyoto, Japan) in a wavelength range of 400–800 nm. A microwave photoconductivity decay system (WT-2000 μPCD , Semilab, Budapest, Hungary) was applied to measure the minority carrier lifetime of solar cells.

3. Results

The Si substrate was immersed in diluted NaOH aqueous solution for 5, 15, 30, 45, and 60 min, separately. The J–V curves under illumination of AM (air mass) 1.5 G light in dark conditions are illustrated in Figure 1. The major performance parameters obtained from Figure 1a are summarized in Table 1, and the major performance changes in immersion time are presented in Figure 2. As Table 1 illustrates, the solar/-H device yielded a PCE of 10.01% with short-circuit current density (J_{sc}) of 33.24 mA/cm^2 , V_{oc} of 553 eV, and fill factor (FF) of 53.6%. When the Si was immersed in the diluted NaOH aqueous for 15 min, the optimal PCE, J_{sc} , and FF for solar/-OH(15) were 12.05%, 34.95 mA/cm^2 , and 61.73%, respectively, with a slightly increased V_{oc} of 559 eV. The solar/-OH(15) device presented relatively higher J_{sc} and FF than the solar/-H device, resulting in an increase of PCE from 10.01% to 12.05%.

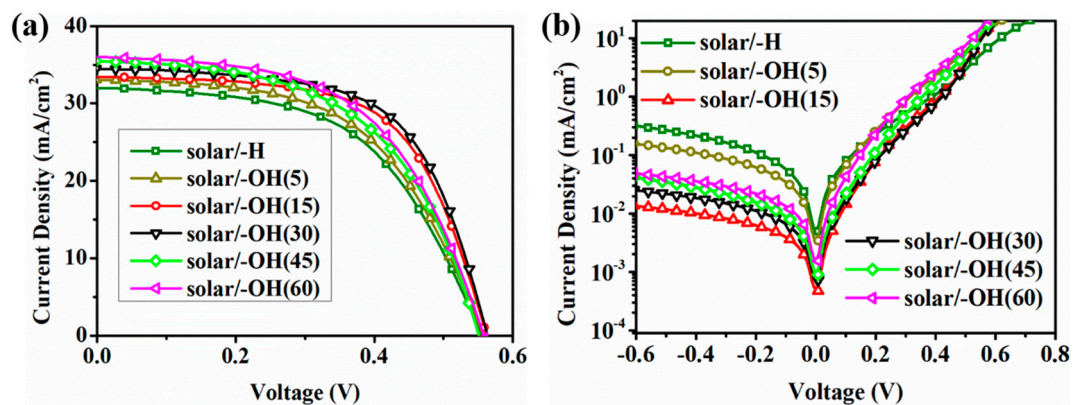


Figure 1. J–V curves of PEDOT:PSS/Si solar cells with different immersion times: (a) under illumination of AM 1.5 G light, (b) under dark.

Table 1. Major performance parameters of PEDOT:PSS/Si solar cells (the number in parentheses represents performance parameters of the most optimal device).

Performance Parameter	PCE (%)	V_{oc} (eV)	J_{sc} (mA/cm ²)	FF (%)
solar/-H	9.4 ± 0.7 (10.01)	556 ± 3 (553)	32.4 ± 0.7 (33.24)	48.9 ± 3.2 (53.6)
solar/-OH(5)	10.4 ± 0.6 (11.04)	555 ± 3 (556)	33.1 ± 1.0 (33.56)	56.7 ± 4.3 (59.2)
solar/-OH(15)	11.3 ± 0.6 (12.05)	559 ± 3 (559)	33.9 ± 1.0 (34.95)	59.5 ± 2.4 (61.73)
solar/-OH(30)	11.1 ± 0.6 (11.98)	560 ± 7 (555)	34.7 ± 0.7 (35.67)	58.1 ± 3.6 (60.58)
solar/-OH(45)	10.7 ± 0.9 (11.10)	553 ± 2 (555)	34.4 ± 1.0 (35.48)	56.4 ± 3.7 (58.91)
solar/-OH(60)	10.3 ± 0.8 (10.83)	556 ± 3 (555)	36.0 ± 1.5 (36.29)	55.1 ± 3.9 (55.23)

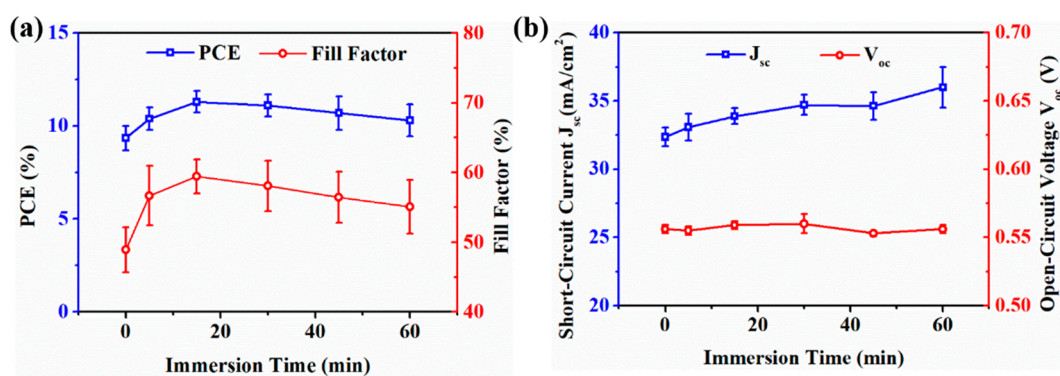


Figure 2. Major performance parameters versus immersion time: (a) PCE and FF; (b) J_{sc} and V_{oc} .

As shown in Figure 2a, the PCE of prepared devices improved until the immersion time reached 15 min, then declined as immersion time increased, which indicated that immersion time significantly influenced the PCE when exceeding 15 min. The FF improved to 61.73% when immersion time was 15 min, and dropped to 55.23% at 60 min. Per Figure 2b, the J_{sc} of the prepared device continuously increased with longer immersion time, whereas the V_{oc} was nearly unchanged with immersion time varying. Thus, the PCE, J_{sc} , and FF of the device were greatly affected when the Si substrate was immersed in diluted NaOH aqueous solution for different periods of time. The improved PCE of the

devices mainly occurred due to the enhancement of FF and J_{sc} at 15 min; the PCE increased 19.3% compared to the device without diluted NaOH aqueous solution processing.

The surface was terminated with $-OH$ when the Si substrate was processed with diluted NaOH aqueous solution [27–29]. This benefited the surface wettability of Si substrate, which might help modify the quality of junction formed by the PEDOT: PSS and Si substrate. As shown in Figure 2a, the FF improved when immersion time was less than 15 min, and reached the highest value at 15 min. The FF was minimized when immersion time was longer than 15 min. Such evolution indicates that the junction quality was optimized when Si substrate was processed with diluted NaOH aqueous solution, and that the most optimal immersion time was 15 min. The dark J–V test and EIS were effective in exploring the junction quality. In Figure 1b, the change trend of dark J–V curves for different immersion times was in consistent with the FF in Figure 2a.

The measured and fitted Nyquist plots of devices prepared with different immersion times is presented in Figure 3a, and the inset is the equivalent circuit model for the spectra fitting (R_s : series resistance, R_{rec} : recombination resistance, and C_1 : junction capacitance). The impedance spectra for the devices was nearly semicircular, proving that only a single junction formed in the devices. The heights and diameters of spectra for different immersion times continuously increased until immersion time reached 15 min, then decreased as immersion time increased. Such observations are related to the recombination resistance (R_{rec}) and the junction capacitance (C_1). To provide a full understanding of the EIS test results, fitting the data with an equivalent circuit model (inset in Figure 3a) was necessary. The model contained a parallel connected $R_{rec}-C_1$ network and a series resistance (R_s) serially connected to the $R_{rec}-C_1$ network. The fitted parameters are presented in Table 2.

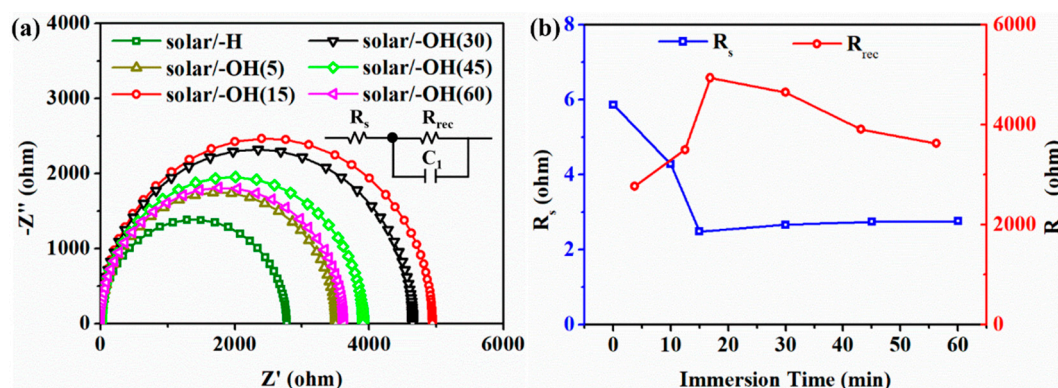


Figure 3. Electrochemical impedance spectra test results and fitted parameters of the equivalent circuit model: (a) Nyquist plots, the scatters are the experiment data and the solid line is the fitted results; (b) fitted parameters.

Table 2. Impedance characteristics of the tested devices.

Device	R_s (ohm)	R_{rec} (ohm)	C_1 (F)	τ (μs)
solar/-H	5.872	2770	1.33×10^{-7}	368.41
solar/-OH(5)	4.284	3500	1.39×10^{-7}	486.5
solar/-OH(15)	2.489	4938	1.33×10^{-7}	656.75
solar/-OH(30)	2.667	4647	1.36×10^{-7}	631.99
solar/-OH(45)	2.749	3907	1.35×10^{-7}	527.45
solar/-OH(60)	2.758	3626	1.32×10^{-7}	478.63

R_s in Figure 3b exhibited a decrease until immersion time reached 15 min, then slightly increased as immersion time increased. The R_{rec} increased with immersion time, and reached the highest value at 15 min, then decreased as immersion time increased. The R_{rec} is also an important parameter related to device performance because high R_{rec} helps to diminish the possibility of carrier recombination and suppresses the leakage current at the junction. A lower R_s indicates the suppression of the drift current

at the junction under dark conditions and the minimization of the reverse saturation current. For solar cells, the dark current contains the reverse saturation current and leakage current. Thus, reduced R_s and increased R_{rec} contribute to minimizing reverse saturation current and leakage current, leading to decreased dark current, as Figure 1b illustrates, and improvement in junction quality. The carrier recombination of the device prepared under 15 min immersion was greatly depressed, and the carrier separation was encouraged, which benefited the performance improvement of the device (especially the FF).

The minor carrier lifetime (τ) of the prepared device could be obtained based on the relationship between R_{rec} and C_1 [19,30]; the calculated results are presented in Table 2. A higher τ indicates that an enhanced carrier separation at the interface, and that the carrier recombination is suppressed. The evolution of τ with different immersion times was found to be in accordance with the R_{rec} , and the highest value of τ was observed at 15 min immersion. To further explore the effectiveness of diluted NaOH aqueous solution in helping to suppress carrier recombination and enhance the junction quality, the minor carrier lifetime was directly measured with a microwave photoconductivity decay system, and the results are presented in Figure 4. The average minority carrier lifetime for solar/-H and solar/-OH(15) were 7.85 and 12.47 μ s, respectively, which is in agreement with the evolution trend of minor carrier lifetime obtained from the Nyquist plots. Thus, processing the Si substrate with diluted NaOH aqueous solution contributed to the optimization of the junction quality of the prepared device, and 15 min was the most optimal immersion time.

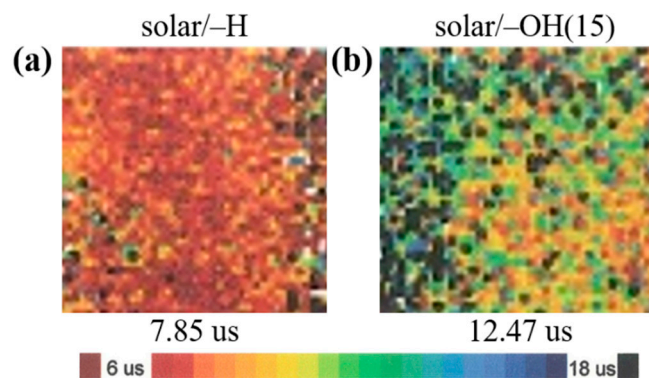


Figure 4. Mappings of minority carrier lifetime for two kinds of devices: (a) solar/-H; (b) solar/-OH(15).

Apart from the improved FF when processing with diluted NaOH aqueous solution, the J_{sc} was also modified according to the results in Table 1 and Figure 2b. The surface of the Si substrate would be etched when immersed in NaOH aqueous solution [7], which might be the reason for the improvement in J_{sc} . Thus, it was necessary to explore the surface morphology of the Si substrate. Figure 5 presents the AFM test results after the Si substrate was immersed in diluted NaOH aqueous solution for 0, 15, and 60 min. The RMS value of the Si surface increased from 0.76 to 5.57 nm after being immersed in diluted NaOH aqueous solution. As shown in Figure 5b, many micro-structures on the surface were formed after 15 min of immersion, and the surface became much rougher than the surface without immersion. The etched micro-structures on the Si surface promoted light harvesting. Figure 6a illustrates the EQE spectra of solar/-H and solar/-OH(15). The EQE spectra of solar/-OH(15) was higher than solar/-H among spectral regions from 450 and 850 nm, which echoed the results from reflectance spectra in Figure 6b. The reflection spectra proved that the light harvesting ability of bare Si after 15 min immersion was enhanced, which meant more photons would be used to produce carriers in the Si substrate. The EQE spectra revealed that the carrier separation was more efficient after 15 min immersion, proving that more carriers would be separated efficiently at the device interface. Thus, the J_{sc} improvement was due to the enhanced light harvesting ability of Si substrate originating from the surface etching, and efficient carrier separation resulted from the improved junction quality. Although a much rougher Si substrate surface would improve the light trapping and J_{sc} , more recombination

centers were introduced in the device, resulting in decreased FF, as Figure 2a illustrates, and poor junction quality.

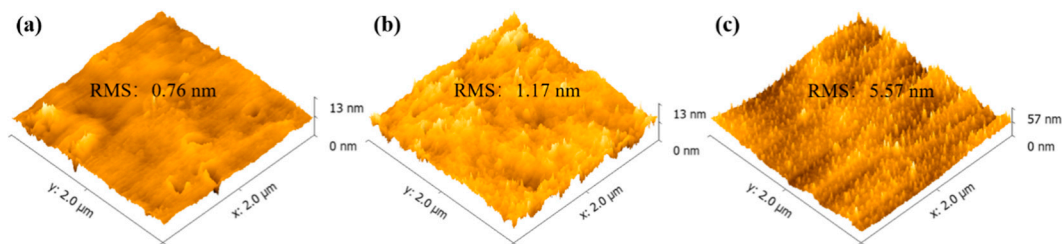


Figure 5. AFM testing results of Si substrate (a) without diluted NaOH aqueous immersion, (b) with 15 min diluted NaOH aqueous immersion, and (c) with 60 min diluted NaOH aqueous immersion.

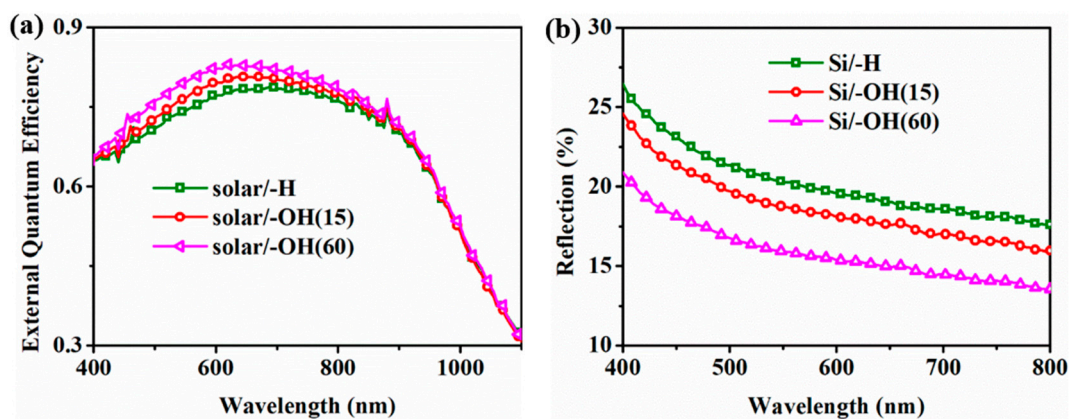


Figure 6. The EQE and reflection spectra: (a) EQE spectra of prepared devices; (b) reflection spectra of bare Si.

Based on the discussion above, the major effects of diluted NaOH aqueous solution treatment for Si substrate included etching the surface and terminating the surface with $-OH$ as Figure 7 illustrating. Such effects benefit the light trapping ability and wettability of bare Si. The improved wettability can facilitate better junction quality, enhancing the carrier separation at the interface as a result. Both the improved light trapping ability of bare Si and the better junction quality contribute to the production of more carriers and facilitate the carrier separation efficiently. In other words, more photons were converted to charge carriers, which were then separated efficiently at the junction, leading to the improvements in J_{sc} , FF and PCE performance of PEDOT: PSS/Si solar cells. Excessive etching produced more minor structures, which means more recombination centers were introduced at the interface between the PEDOT: PSS and the Si substrate. As shown in Figure 5c, the Si surface became rougher and more micro-structures were formed when immersion time reached 60 min. As reported [3,13], the PEDOT: PSS film could not cover the Si surface with micro-structures very well, which led to poor junction quality, as Figure 3 illustrates. Many recombination centers formed, and the carrier recombination was enhanced. The poor junction quality of the device led to decreased R_{rec} and increased R_s , causing FF to drop despite the improved J_{sc} presented in Figure 2. The PCE with an immersion time of 60 min was smaller than the device prepared with an immersion time of 15 min. Thus, the Si surface needed to be properly processed with diluted NaOH aqueous solution, and 15 min immersion was the most suitable processing time in this study.

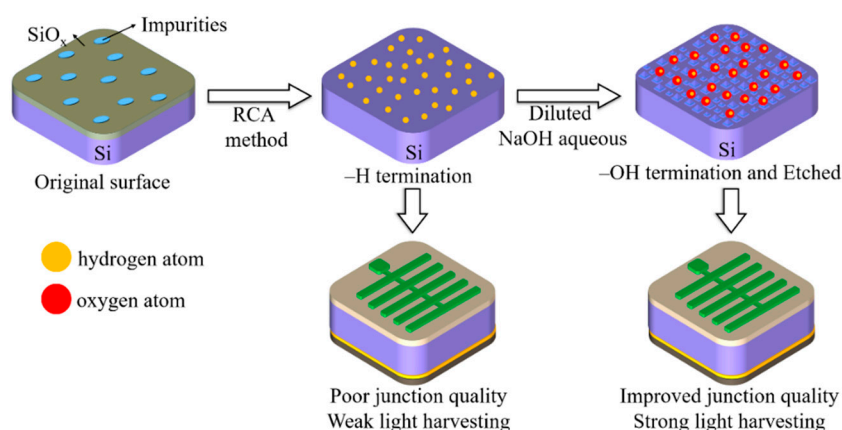


Figure 7. Influence of diluted NaOH aqueous on Si surface.

4. Conclusions

This paper proposed and proved that the proper processing of Si substrate with diluted NaOH aqueous solution is an efficient and convenient method to improve the performance of Si/PEDOT:PSS solar cells. When Si substrate was immersed in diluted NaOH aqueous solution for different amounts of time, the PCE and FF of the devices improved until the immersion time reached 15 min, then decreased as immersion time increased. This trend was consistent with the junction quality analysis obtained from the dark J–V and EIS measurements. The J_{sc} continued rising as immersion time increased. The improvement of J_{sc} was due to the light trapping ability enhancement of the Si substrate with etched surface. Thus, the enhanced light trapping ability meant more photons could be converted to charge carriers, and optimized junction quality could suppress the carrier recombination and facilitate the carrier separation. In this way, the performance of PEDOT:PSS/Si solar cells improved. The most optimal immersion time was 15 min, when the PCE of prepared Si/PEDOT:PSS solar cell rose to 12.05% with a J_{sc} of 34.95 mA/cm², V_{oc} of 559 eV, and FF of 61.73%. In conclusion, processing Si substrate with diluted NaOH aqueous solution can promote the efficiency of Si/PEDOT:PSS solar cells with low-cost fabrication technologies.

Author Contributions: Experimental work, T.C. and H.G.; result evaluation and manuscript preparation, T.C.; figure preparing and modification, T.C. and L.Y.; review and editing, T.S. and Y.Y. All authors have read and agreed to the published version of the manuscript.

Funding: This research was funded by Construction Fund of International Joint Research Centre for Optoelectronic and Energy Materials by Yunnan Provincial Department of Finance (No. 2017IB033), the Yunnan University Action Plan of Serve the Yunnan Province (No. 2016MS15) and Yunling Scholars Fund of Yunnan Ten Thousand Talents Program (No. KC194317).

Conflicts of Interest: The authors declare no conflict of interest.

References

1. Shiu, S.-C.; Chao, J.-J.; Hung, S.-C.; Yeh, C.-L.; Lin, C.-F. Morphology Dependence of Silicon Nanowire/Poly (3,4-Ethylenedioxythiophene):Poly (Styrenesulfonate) Heterojunction Solar Cells. *Chem. Mater.* **2010**, *22*, 3108–3113. [[CrossRef](#)]
2. Zielke, D.; Pazidis, A.; Werner, F.; Schmidt, J. Organic-Silicon Heterojunction Solar Cells on N-Type Silicon Wafers: The Backpedot Concept. *Sol. Energy Mater. Sol. Cells* **2014**, *131*, 110–116. [[CrossRef](#)]
3. Yang, Z.; Gao, P.; He, J.; Chen, W.; Yin, W.Y.; Zeng, Y.; Guo, W.; Ye, J.; Cui, Y. Tuning of the Contact Properties for High-Efficiency Si/PEDOT:PSS Heterojunction Solar Cells. *ACS Energy Lett.* **2017**, *2*, 556–562. [[CrossRef](#)]
4. Wang, H.; Wang, J.; Rusli. Hybrid Si Nanocones/PEDOT:PSS Solar Cell. *Nanoscale Res. Lett.* **2015**, *10*, 191. [[CrossRef](#)] [[PubMed](#)]
5. Bhujel, R.; Swain, B.P. Fabrication and Characterization of Silicon Nanowires Hybrid Solar Cells: A Review. *IOP Conf. Ser. Mater. Sci. Eng.* **2018**, *377*, 012193. [[CrossRef](#)]

6. Thomas, J.P.; Leung, K.T. Defect-Minimized PEDOT:PSS/Planar-Si Solar Cell with Very High Efficiency. *Adv. Funct. Mater.* **2014**, *24*, 4978–4985. [[CrossRef](#)]
7. Yoon, S.-S.; Khang, D.-Y. Ag Nanowire/ PEDOT:PSS Bilayer Transparent Electrode for High Performance Si-PEDOT:PSS Hybrid Solar Cells. *J. Phys. Chem. Solids* **2019**, *129*, 128–132. [[CrossRef](#)]
8. Zhu, J.; Yang, X.; Yang, Z.; Wang, D.; Gao, P.; Ye, J. Achieving a Record Fill Factor for Silicon-Organic Hybrid Heterojunction Solar Cells by Using a Full-Area Metal Polymer Nanocomposite Top Electrode. *Adv. Funct. Mater.* **2018**, *28*, 1705425. [[CrossRef](#)]
9. Fan, Q.; Zhang, Q.; Zhou, W.; Xia, X.; Yang, F.; Zhang, N.; Xiao, S.; Li, K.; Gu, X.; Xiao, Z.; et al. Novel Approach to Enhance Efficiency of Hybrid Silicon-Based Solar Cells Via Synergistic Effects of Polymer and Carbon Nanotube Composite Film. *Nano Energy* **2017**, *33*, 436–444. [[CrossRef](#)]
10. Cui, W.; Wu, S.; Chen, F.; Xia, Z.; Li, Y.; Zhang, X.; Song, T.; Lee, S.; Sun, B. Silicon/Organic Heterojunction for Photoelectrochemical Energy Conversion Photoanode with a Record Photovoltage. *ACS Nano* **2016**, *10*, 9419. [[CrossRef](#)]
11. Young, J.; Shin, M.; Lee, J.B.; Ahn, J.H.; Baik, H.K.; Jeong, U. Effect of Pedot Nanofibril Networks on the Conductivity, Flexibility, and Coatability of Pedot: Pss Films. *ACS Appl. Mater. Interfaces* **2014**, *6*, 6954–6961.
12. Singh, P.; Sanjay, K.; Srivastava, B.; Sivaiah, P.; Prathap, C.; Rauthan, M.S. Enhanced Photovoltaic Performance of Pedot:Pss/Si Solar Cells Using Hierarchical Light Trapping Scheme. *Sol. Energy* **2018**, *170*, 221–233. [[CrossRef](#)]
13. Wang, Y.; Shao, P.; Chen, Q.; Li, Y.; Li, J.; He, D. Nanostructural Optimization of Silicon/PEDOT:PSS Hybrid Solar Cells for Performance Improvement. *J. Phys. D Appl. Phys.* **2017**, *50*, 175105. [[CrossRef](#)]
14. Zhang, L.; Wang, Z.; Lin, H.; Wang, W.; Wang, J.; Zhang, H.; Sheng, J.; Wu, S.; Gao, P.; Ye, J. Thickness-Modulated Passivation Properties of PEDOT:PSS Layers over Crystalline Silicon Wafers in Back Junction Organic/Silicon Solar Cells. *Nanotechnology* **2019**, *30*, 195401. [[CrossRef](#)]
15. Wu, S.; Cui, W.; Aghdassi, N.; Song, T.; Duhm, S.; Lee, S.T.; Sun, B. Nanostructured Si/Organic Heterojunction Solar Cells with High Open-Circuit Voltage Via Improving Junction Quality. *Adv. Funct. Mater.* **2016**, *26*, 5035–5041. [[CrossRef](#)]
16. He, J.; Wan, Y.; Gao, P.; Tang, J.; Ye, J. Over 16.7% Efficiency Organic-Silicon Heterojunction Solar Cells with Solution-Processed Dopant-Free Contacts for Both Polarities. *Adv. Funct. Mater.* **2018**, *28*, 1802192. [[CrossRef](#)]
17. He, L.; Jiang, C.; Wang, H.; Lai, D.; Rusli. High Efficiency Planar Si/Organic Heterojunction Hybrid Solar Cells. *Appl. Phys. Lett.* **2012**, *100*, 073503. [[CrossRef](#)]
18. Zhang, C.; Zhang, Y.; Guo, H.; Jiang, Q.; Dong, P.; Zhang, C. Efficient Planar Hybrid n-Si/ PEDOT:PSS Solar Cells with Power Conversion Efficiency up to 13.31% Achieved by Controlling the SiO_x Interlayer. *Energies* **2018**, *11*, 1397. [[CrossRef](#)]
19. Nam, Y.-H.; Song, J.-W.; Park, M.-J.; Sami, A.; Lee, J.-H. Ultrathin Al₂O₃ Interface Achieving an 11.46% Efficiency in Planar n-Si/ PEDOT:PSS Hybrid Solar Cells. *Nanotechnology* **2017**, *28*, 155402. [[CrossRef](#)]
20. Liu, Y.; Zhang, J.; Wu, H.; Cui, W.; Wang, R.; Ding, K.; Lee, S.-T.; Sun, B. Low-Temperature Synthesis TiO_x Passivation Layer for Organic-Silicon Heterojunction Solar Cell with a High Open-Circuit Voltage. *Nano Energy* **2017**, *34*, 257–263. [[CrossRef](#)]
21. Yadav, T.S.; Sharma, A.K.; Kottantharayil, A.; Basu, P.K. Comparative Study of Different Silicon Oxides Used as Interfacial Passivation Layer (SiNy:H/SiO_x/n+-Si) in Industrial Monocrystalline Silicon Solar Cells. *Sol. Energy Mater. Sol. Cells* **2019**, *201*, 110077. [[CrossRef](#)]
22. Kern, W. The Evolution of Silicon Wafer Cleaning Technology. *J. Electrochem. Soc.* **1990**, *137*, 1887–1892. [[CrossRef](#)]
23. Untila, G.G.; Kost, T.N.; Chebotareva, A.B. F-In-Codoped ZnO (FiZO) Films Produced by Corona-Discharge-Assisted Ultrasonic Spray Pyrolysis and Hydrogenation as Electron-Selective Contacts in FiZo/SiO/p-Si Heterojunction Crystalline Silicon Solar Cells with 10.5% Efficiency. *Sol. Energy* **2019**, *181*, 148–160. [[CrossRef](#)]
24. Pollock, K.L.; Junge, J.; Hahn, G. Detailed Investigation of Surface Passivation Methods for Lifetime Measurements on P-Type Silicon Wafers. *IEEE J. Photovolt.* **2011**, *2*, 1–6. [[CrossRef](#)]
25. Dixit, P.; Chen, X.; Miao, J.; Divakaran, S.; Preisser, R. Study of Surface Treatment Processes for Improvement in the Wettability of Silicon-Based Materials Used in High Aspect Ratio through-Via Copper Electroplating. *Appl. Surf. Sci.* **2007**, *253*, 8637–8646. [[CrossRef](#)]

26. Song, J.-W.; Nam, Y.-H.; Park, M.-J.; Shin, S.-M.; Wehrspohn, R.B.; Lee, J.-H. Hydroxyl Functionalization Improves the Surface Passivation of Nanostructured Silicon Solar Cells Degraded by Epitaxial Regrowth. *RSC Adv.* **2015**, *5*, 39177–39181. [[CrossRef](#)]
27. Allongue, P.; Kieling, V.C.; Gerischer, H. Etching of Silicon in NaOH Solutions I. In Situ Scanning Tunneling Microscopic Investigation of n-Si(111). *J. Electrochem. Soc.* **1993**, *140*, 1009–1018. [[CrossRef](#)]
28. Allongue, P.; Kieling, V.C.; Gerischer, H. Etching of Silicon in NaOH Solutions II. Electrochemical Studies of n-Si(111) and (100) and Mechanism of the Dissolution. *J. Electrochem. Soc.* **1993**, *140*, 1018–1026. [[CrossRef](#)]
29. Bressers, P.M.M.C.; Kelly, J.J.; Gardeniers, J.G.E.; Elwenspoek, M. Surface Morphology of p-Type (100) Silicon Etched in Aqueous Alkaline Solution. *J. Electrochem. Soc.* **1996**, *143*, 1744–1750. [[CrossRef](#)]
30. Hu, W.; Xu, C.Y.; Niu, L.B.; Elseman, A.M.; Wang, G.; Liu, B.; Yao, Y.Q.; Liao, L.P.; Zhou, G.D.; Song, Q.L. High Open-Circuit Voltage of 1.134 V for Inverted Planar Perovskite Solar Cells with Sodium Citrate-Doped PEDOT:PSS as a Hole Transport Layer. *ACS Appl. Mater. Interfaces* **2019**, *11*, 22021–22027. [[CrossRef](#)]



© 2020 by the authors. Licensee MDPI, Basel, Switzerland. This article is an open access article distributed under the terms and conditions of the Creative Commons Attribution (CC BY) license (<http://creativecommons.org/licenses/by/4.0/>).